Long Range Neutron-Gamma Point Source Detection and Imaging Using Unique Rotating Detector

Jeffrey L. Lacy, *Member, IEEE*, Athanasios Athanasiades, Christopher S. Martin, Liang Sun, *Member, IEEE*, Jeffry W. Anderson, and Tom D. Lyons

***Abstract*–We propose a new radiation detection technology that offers high sensitivity to both gamma rays and neutrons, and can be applied, cost effectively, to survey monitoring. The detector consists of a close-packed array of many small thin-walled copper straws, each 1 m in length, and lined with a very thin (1 μm) coating of enriched boron carbide ($^{10}B_4C$). Gammas are converted in Cu, while thermal neutrons are converted in ^{10}B. The detector design draws upon low-cost technology developed by the high energy physics community for large particle detectors such as ATLAS, currently being commissioned at CERN. The feasibility of the detection technology has been demonstrated previously [1], [2]. The current work presents a unique application of the straw detectors, whereby a rotating panel is used to significantly improve performance. The proposed concept is based on the characteristic signature of a point source, that differentiates it from background noise. We present and evaluate an algorithm for detecting the presence of a source and estimating its net count, direction, and the background rate. Simulation results show that the proposed technique can detect in about 20 minutes time and in an area 100 m in diameter, a 1 mCi gamma ray source, with 90% sensitivity and false alarm probability of 0.1/hour. At 30 min time, 270 g of neutron-emitting ^{240}Pu can be detected within a circular area 100 m in diameter, assuming 20% of neutrons thermalize near the source.**

I. Introduction

We present a technique for passive, long-range detection and localization of gamma and neutron emitting sources, based on the unique signature of a point source, that differentiates it from background noise. Hidden nuclear materials have limited extent, and can be approximated by point sources in a uniform natural background. The method assumes only that the neutron or gamma environmental background is uniform in pointing angle and that the source is small in extent, approximating a point source.

A large area panel of detectors is rotated around its vertical axis, while neutron and gamma counts are recorded at 1 second intervals. Operating in this mode, the panel's angular response (counts vs. rotation angle) exhibits a characteristic shape that can be processed to significantly enhance sensitivity and to deduce the source size and direction.

The technique proposed here requires the use of large panel detectors that are inexpensive to manufacture, sensitive to both neutrons and gammas, lightweight, ruggedized for field application, and safe for portable operation. We present a design that satisfies these requirements, based on straw detector technology previously applied to a portable monitor [2] and neutron imaging [1]. The detector consists of a close-packed array of many small thin-walled copper straws, as shown in Fig. 1, each 1 m in length, and lined with a very thin (1 μm) coating of enriched boron carbide ($^{10}B_4C$). Gammas are converted in Cu, while neutrons are converted in ^{10}B. Electrons from gamma interactions and atomic fragments from neutron interactions escape the straw wall and ionize the counting gas contained inside each straw. This ionization is collected to a thin central anode wire where avalanche amplification occurs. The detector design draws upon low-cost technology developed by the high energy physics community for large particle detectors such as ATLAS, currently being commissioned at CERN.

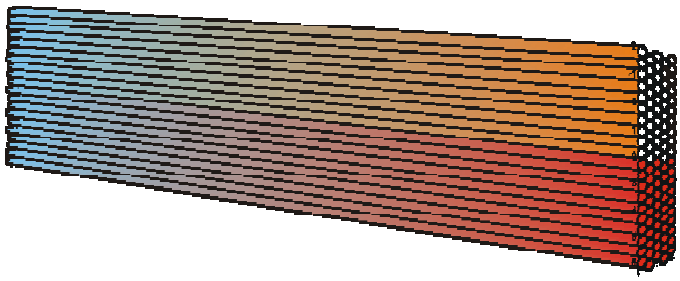

Fig. 1. Array of copper straw detectors, grouped into two modules of 50. Each straw is 1 m in length, and 4 mm in diameter. Many such modules can be combined to form a square-meter panel detector, that is lightweight, safe for portable operation, and sensitive to both neutrons and gamma rays.

The straw detector technology has the following advantages when compared with conventional ^3He-based neutron detectors: 1) sensitivity to both neutrons and gammas, 2) low weight, 3) safety for portable use (no pressurization), 4) low price. In particular, the straw array has the linear stopping power of ^3He gas at a pressure of 2.68 atm, for thermal neutrons, as illustrated in Fig. 2. It is difficult to achieve this pressure safely in portable detectors of the dimension required for long range detection.

A similar gamma source detection technique has been applied in stationary portal monitors, where potential sources travel past the detector [3].

This work is supported by the U.S. Defense Threat Reduction Agency (DTRA).

All authors are with Proportional Technologies, Inc., Houston, TX 77054 USA (telephone: 713-747-7324, e-mail: jlacy@proportionaltech.com).

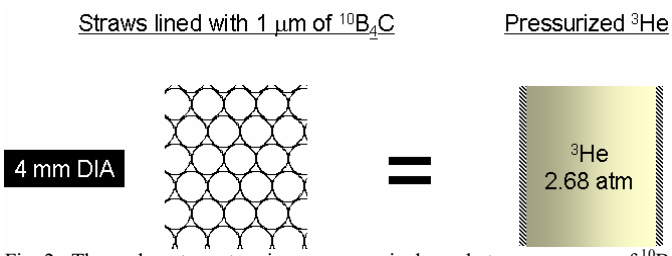

Fig. 2. Thermal neutron stopping power equivalency between an array of ^{10}B-lined straws, and ^{3}He gas.

II. PROPOSED DETECTOR DESIGN

Straw detectors are initially grouped into modules, each housing a close-packed array of 50 straws. The module forms a hermetic seal along the whole length of the meter-long array, and has room for electronic boards, as required for signal readout. Once powered, each module can function as an independent detector with digital outputs for neutron and gamma counts.

All sides of the module are shielded for thermal neutrons, except for the front 100 cm × 4 cm face, which is fitted with a thermal neutron collimator. More details on the housing and collimator designs are presented in the next section.

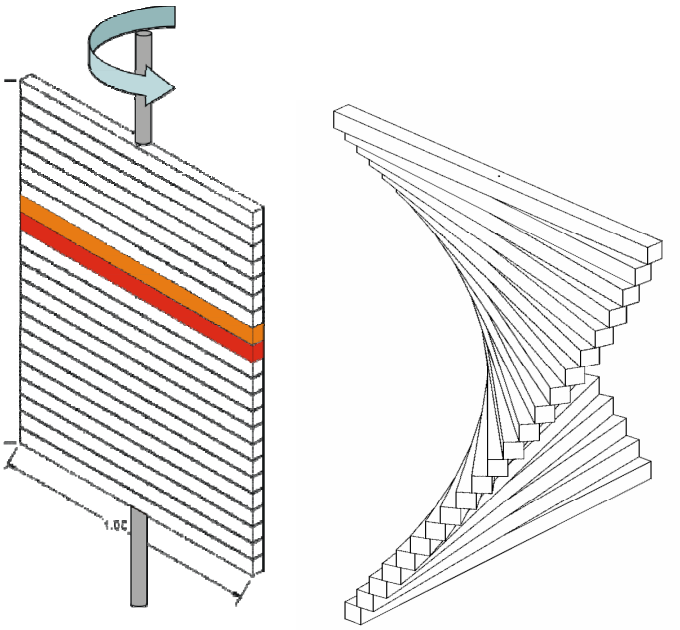

Fig. 3. *left*, Proposed 100 cm × 100 cm × 1.7 cm detector panel, made from a stack of straw modules. Each module contains an array of 50 straw detectors, as shown in Fig. 1. Each straw detector is 1 m long, and 4 mm in diameter. *right*, Alternative configuration, where modules are arranged in a helical pattern, requiring a smaller range of rotation.

Several 50-straw modules are stacked one deep, as shown in Fig. 3, to form a 100 cm × 100 cm panel detector, that is lightweight and safe for portable operation. The panel is supported in a manner that allows it to rotate around its vertical axis, at a rate of 1 revolution per minute, as illustrated in Fig. 4. While the panel rotates, neutron and gamma counts are recorded at 1 second intervals.

Several performance parameters, including neutron and gamma sensitivities, gamma discrimination, and background rates were determined in Monte Carlo simulations, implemented in MCNP5 for the interactions of neutrons, photons and electrons with the detector materials; and in SRIM-2006, for the range of charged particles.

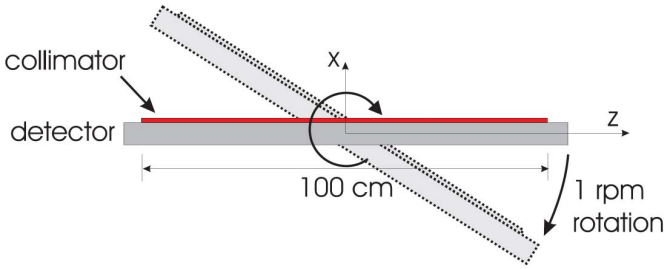

Fig. 4. Top view of the proposed 100 cm × 100 cm × 1.7 cm detector panel. The panel is 100 cm long in the y-direction and rotates around the y-axis. It is shielded on all sides for thermal neutrons, except for the front face which incorporates a 100 cm × 100 cm thermal neutron collimator.

III. METHODS

Fig. 5 shows the kind of net response (background subtracted) that the panel detector of Fig. 3 will demonstrate, for different gamma ray emitting isotopes, and for a neutron emitter, assuming they are point-like in size. These measurements were collected in a small-scale, rotating prototype, shown in Fig. 8, previously developed for homeland security applications [2]. We first present the algorithm developed for the detection and localization of remote point sources in an unknown but azimuthally uniform background, based on the curves of Fig. 5.

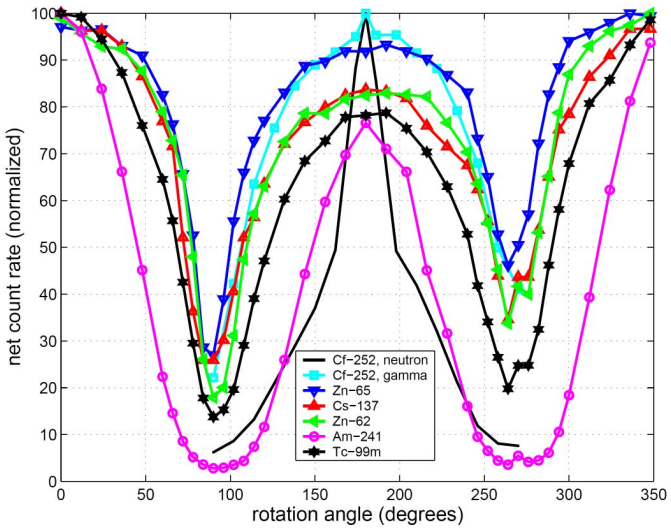

Fig. 5. Net (background subtracted) angular response of a prototype 40 cm × 5 cm × 5 cm monitor to different radiation sources. These data, collected over long times and with nearby sources are used as a template in the algorithm for long range detection.

A. Algorithm for the detection of gamma rays

Assuming that the count rate in the rotating panel is recorded every second, and that data are averaged over the two half-rotations, we have N=30 data points (θ_i, y_i), where θ_i is the rotation angle (0 to 180 degrees), and y_i is the measured gamma count rate, with i=1..30. We would like to estimate the

component of y_i that is due to the gamma ray background, and the component that is due to a gamma point source that may be present. In addition, we want to identify the source direction. In order to achieve these objectives, we assume that the data y_i equal an analytical expression f_i, such that $y_i=f_i$, and that

$$f_i = (\text{net signal})_i + (\text{background})_i \quad (1)$$

It can be shown (see Appendix) that

$$f_i = a \cdot yt_i / \Sigma(yt_i) + (\Sigma(y_i)-a) \cdot (1/30), \quad (2)$$

where $yt_i = yt_i(\theta_i+b)$ is the known net angular response of the detector, depicted in Fig. 5, for each angle θ_i+b. We now need to estimate constants a and b. To do that, we compute and then minimize the χ^2 function, written as

$$\chi^2 = \Sigma \, (y_i - f_i(\theta_i,a,b))^2 / y_i \qquad \text{for i=1 to 30} \quad (3)$$

Once we have a_0 and b_0 for which $\chi^2(a_0,b_0)=\min(\chi^2)$, then we can evaluate the following quantities, using (2):

- the net signal (averaged over all angles) equals $a_0/30$;
- the background rate equals $(\Sigma(y_i)-a_0)/30$;
- and the source direction angle equals b_0.

B. Algorithm for the detection of neutrons

The neutron algorithm follows the general development presented above for gamma rays, however, because neutron counts follow a Poisson rather than a normal distribution, the function minimized is the negative logarithm of the Likelihood Function,

$$\begin{aligned} -\ln(L) &= -\ln (\Pi \, e^{-fi} \cdot f_i^{yi} / y_i!) \\ &= \Sigma \, f_i - \Sigma \, (y_i \ln(f_i)) + \ln(\Pi \, y_i!) \end{aligned} \quad (4)$$

C. Detection limits

We have evaluated the performance of the algorithm, applied to the rotating panel detector of Fig. 3. Using Monte Carlo simulations of the detector angular response (implemented in MCNP5), and assuming a specific background rate (BG) and measurement time (T), we estimated the minimum detectable signal, for a desired true positive and false alarm probability.

Initially, the detector angular response was simulated for 10,000 repeated background runs, assuming a background rate BG, and a measurement time T. The fitting algorithm described above was employed to estimate the amount of net signal S present in the data (ideally centered around zero). A distribution of 10,000 S values was thus created. The critical value Sc (detection threshold) was established, such that the probability that S>Sc equaled the desired false alarm probability.

Additionally, the detector angular response was simulated for 1,000 different source+background runs, assuming a certain source activity, and the same BG and T as above. The fitting algorithm was employed again to estimate the amount of net signal S present in the data. A second distribution of S was thus generated, and it was checked against the critical value Sc obtained earlier. If S was greater than Sc with a probability of 90%, then the mean of the distribution was set as the minimum detectable signal (MDS). If not, then the simulation was repeated with a higher source activity, until the 90% probability was achieved.

The false alarm probability (FAP) was set to 1 false alarm every 10 hours. For the first 30 minutes, one-minute long collections were successively added, so that the measurement times were T=1 min, 2 min, 3 min, and so forth, up to 30 minutes. We defined a variable FAP equal to FAP=T/600, so that the false alarm rate remained constant at 1 every 10 hours. Beyond a time of 30 minutes, the false alarm probability remained fixed at 30/600=0.05. The algorithm discarded data that were older than 30 minutes.

D. MDS vs. distance

The relationship between the minimum detectable activity A and the distance d between the source and the detector was evaluated as:

$$A = f_{air} \cdot (MDS/So) \cdot (d/do)^2 \cdot Ao$$

where So is the signal measured with the detector using a source of activity Ao at a distance do, f_{air} is a correction factor for the attenuation of gammas in air (evaluated in MCNP5), and MDS is the minimum detectable signal that can be detected with a 90% probability and at the specified FAP and measurement time.

IV. Small-scale prototype detector

We have investigated the validity of the method in a prototype detector that uses that same technology described earlier, with the following exceptions: the prototype straws use natural rather than enriched boron, and have thus limited neutron detection efficiency; and the size of the prototype was 40 cm × 5 cm × 5 cm, significantly smaller than the square meter panel proposed.

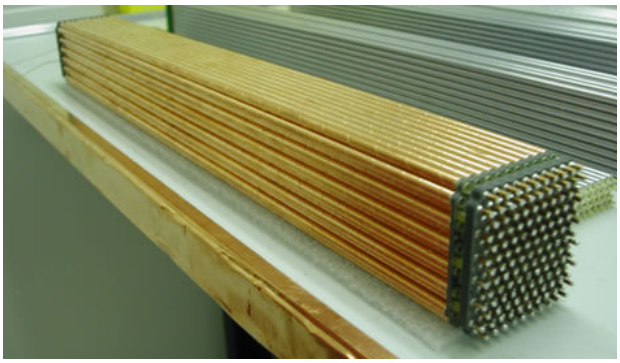

Fig. 6. A small-scale prototype detector was used to evaluate the source detection and localization algorithm. The prototype consisted of 136 B_4C-lined copper straws, each 40 cm long and 4 mm in diameter.

The prototype detector consisted of 136 B_4C-lined copper straws, as shown in Fig. 6, each 40 cm long and 4 mm in

diameter. The straw array was sealed inside a stainless steel housing, which was subsequently evacuated and filled with a gas mixture of 90% argon and 10% methane, at 1 atm. A 2 mm thick thermal neutron shield made of borated aluminum (4.5% boron, ^{10}B-enriched to >95%) was installed on all sides of the housing, except the side where a collimator was fitted, as shown in the diagram of Fig. 7.

The neutron collimator was made up of aluminum straws, of the same diameter as the straws making up the detector module (4 mm), but only 10 mm in length. Collimation is achieved through neutron absorption in ^{10}B-enriched boron carbide ($^{10}B_4C$), incorporated into the wall of each straw. Unlike the detector straws, the collimator straws incorporate a much thicker boron carbide coating, in order to efficiently collimate incident neutrons.

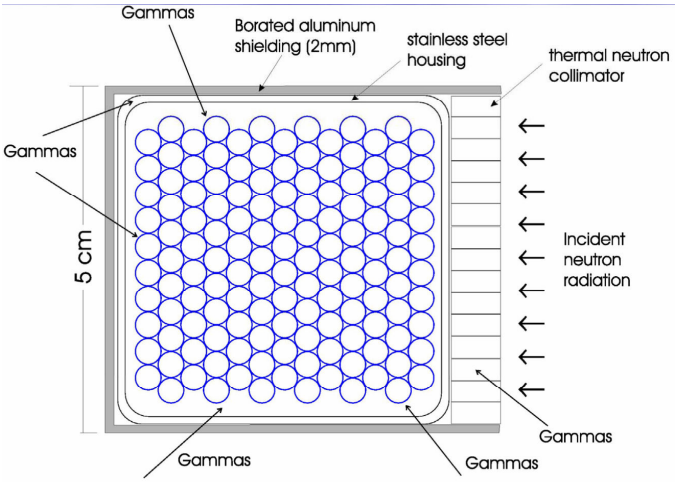

Fig. 7. Cross-sectional diagram of the small-scale prototype and stainless steel housing.

The monitor was read out with a single charge sensitive amplifier (all straw wires were connected together), shaper and discriminator, all sealed inside the detector housing, and an external, dual counter, that incorporated a digital display and control buttons. A built-in high voltage supply biased the straw wires (anode) to 1000 V. A 9 V rechargeable lithium-ion battery powered all electronics and the detector.

Several performance parameters of the small-scale prototype monitor have been published in [2], and are listed in Table I.

A. Detection/localization experiments with small-scale prototype

The proposed neutron and gamma detection and localization method was tested in laboratory experiments, with the prototype monitor mounted on a portable cart, shown in Fig. 8, with motorized 360-degree rotation. A 1-mCi ^{65}Zn gamma ray source was used, hidden in various locations inside the laboratory area. The source was positioned at various distances away from the detector, and at different direction angles, behind walls and laboratory furniture or equipment. A 0.37 μg ^{252}Cf neutron source, equivalent to 0.94 kg of ^{240}Pu was used in additional experiments following the same design. In order to achieve neutron thermalization, the source was placed inside a polyethylene cylinder with a 10 cm diameter.

TABLE I
SMALL-SCALE PROTOTYPE DETECTOR PERFORMANCE

Effective dimensions	40 cm × 5 cm × 5 cm
Number of 40-cm straws	136
Weight (incl. housing, shield)	3.7 kg
Neutrons	
Background rate	0.03 cps
Sensitivity (thermal)	36 cps/nv
Detection efficiency (thermal)	18%
Gammas	
Background rate	20-25 cps
Sensitivity (662 keV)	251 cpm/(μrem/hr)
Detection efficiency (662 keV)	2.7%

As the detector was rotated at a rate of 1 rpm, the count rate was recorded and binned into 1-second long measurements, corresponding to 60 distinct angle steps. Measurements were carried out for several minutes, then the collected data were processed with the algorithm.

Fig. 8. An aluminum cart was used to support the prototype detector during experiments, and to enable motorized rotation.

V. RESULTS

The performance of the proposed panel detector of Fig. 3 was determined in computer simulations, combined with extrapolations of the performance of the small-scale prototype. Table II summarizes the results.

TABLE II
ESTIMATED PERFORMANCE OF PROPOSED DETECTOR

Effective dimensions	100 cm × 100 cm × 1.7 cm
Number of 1-m long straws	25 × 50
Weight	38 kg
Neutrons	
Background rate	0.3 cps
Sensitivity (thermal)	3700 cps/nv
Detection efficiency (thermal)	37%
Gamma discrimination	10^7
Gammas	
Background rate	600 cps
Sensitivity (662 keV)	7500 cpm/(μrem/hr)
Detection efficiency (662 keV)	1.8%

A. Sensitivity & natural background

The thermal neutron sensitivity of the proposed detector, assuming it incorporates enriched boron, is 3700 cps/nv, corresponding to a detection efficiency of 37% (sensitive area of 10,000 cm^2). The ^{137}Cs gamma ray sensitivity is 7500 cpm/(μrem/hr), corresponding to a detection efficiency of 1.8%.

Based on extrapolation of the small-scale prototype, the natural background count rate is 0.3 cps for neutrons, and 600 cps for gammas.

B. Gamma discrimination

The gamma discrimination factor was found to be 10^7 in the small-scale prototype. Fig. 9 shows the fraction of both neutron and gamma events detected (efficiency) as a function of the discriminator level (threshold). When counting neutrons, the threshold is set to 2.9 V, as indicated in the figure. At this level, the gamma ray efficiency is about 10^{-7}.

C. Detection limits

Fig. 10 shows the minimum activity of a gamma point source that can be detected with 90% probability, as a function of distance from the proposed detector of Fig. 3. The measurement time and false alarm probability (FAP) are indicated next to each curve. The background rate was assumed to be 600 cps in all cases. The curves account for the attenuation of gammas in air, as explained in Section III.D.

A similar plot has been constructed that characterizes the neutron detection limits of the proposed monitor. Fig. 11 shows the minimum detectable amount of ^{240}Pu that can be detected versus distance, assuming a 20% thermalization at or near the source. The background rate was assumed to be 0.3 cps. It can be seen for example that a circular area with a diameter of 100 meters (an area of 7850 m^2) can be screened for the presence of 250 gm or more of ^{240}Pu in less than 30 minutes.

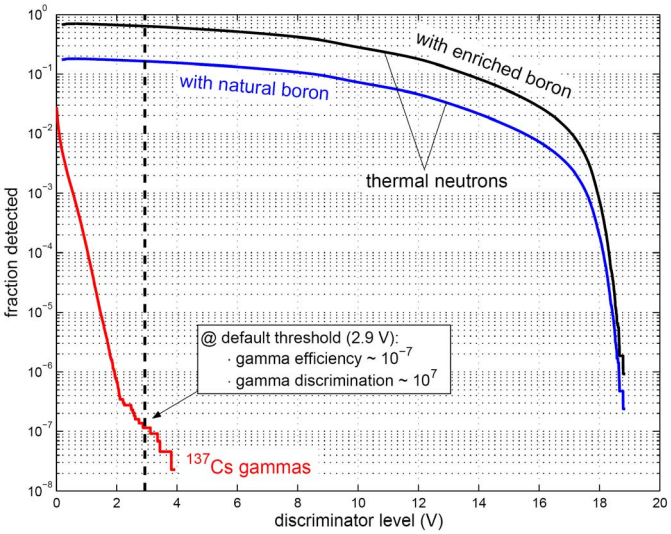

Fig. 9. Neutron-gamma discrimination in the small-scale prototype detector. The variable plotted on the y-axis is the absolute detection efficiency to neutrons and gammas.

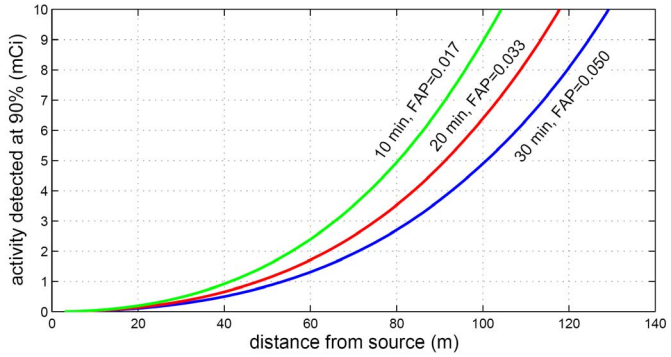

Fig. 10. Estimated minimum detectable activity of a 662 keV gamma ray point source, versus distance, for the rotating monitor of Fig. 2, and for three different measurement times. The sensitivity was 90%. The false alarm probability (FAP) varied with measurement time as indicated, but corresponded to 1 false alarm every 10 hours in all cases.

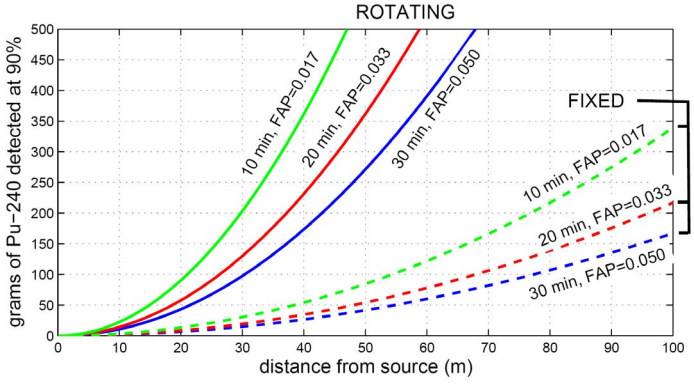

Fig. 11. Estimated minimum detectable amount of ^{240}Pu, versus distance, for the rotating and fixed monitor of Fig. 2, and for three different measurement times. The sensitivity was 90%. The false alarm probability (FAP) varied with measurement time as indicated, but corresponded to 1 false alarm every 10 hours in all cases.

In an alternative detection mode in which a suspected source direction is known so that the detector angle can be fixed the same source can be detected in 2 min.

D. Small-scale prototype experiments

Fig. 12 shows the cumulative counts that the monitor registered over time, in an experiment involving a 1 mCi ^{65}Zn source located 15.8 m away. This signal was processed by the algorithm of Section III to deduce the presence or absence of a radioactive source, calculate its net signal and direction, and the background rate. In this case, a detection was declared after 6 minutes, with a net source signal of 4.8±7.5 cps and a direction of 123±51 degrees. The underlying background was found to be 23±7.6 cps. After accumulating counts over a period of 30 minutes, the source rate changed to 4.6±1.2 cps, the direction to 129±3.6 degrees, and the background to 23±1.2 cps.

A similar experiment involved a 0.37 μg ^{252}Cf neutron source, located 10.2 m away. Fig. 13 shows the cumulative counts. A detection was declared after 3 minutes, with a net source signal of 4.3±1.3 cpm and a direction of 297±19 degrees. The underlying background was 0.022±1.3 cpm. The false alarm probability was set to 1 false alarm every 10 hours, and the true positive probability was set to 90%, as before. For these settings, the detection threshold was 3.8 cpm. After accumulating counts over a period of 30 minutes, the source rate was found to be 1.5±0.80 cpm, the direction was 291±18 degrees, and the background was 2.6±0.81 cpm.

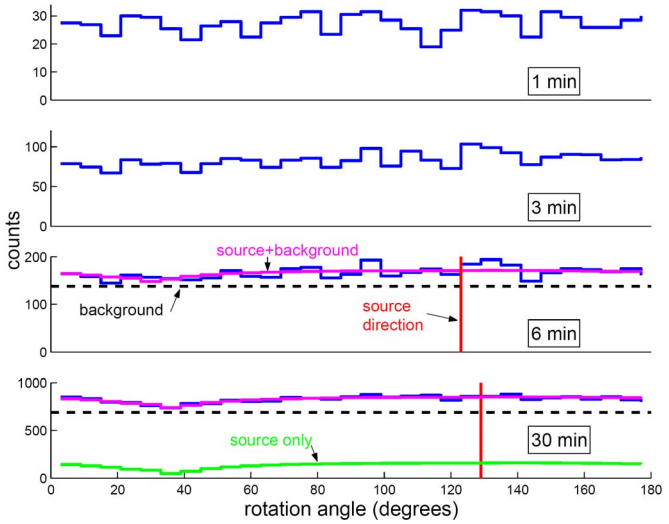

Fig. 12. Cumulative counts collected in the small-scale, rotating monitor, in an experiment involving a 1 mCi ^{65}Zn source located 15.8 m away, and behind walls/furniture. Following processing with the proposed algorithm, a positive detection was first declared at 6 min, for a source located at a direction of 123 degrees (top red line). The false alarm probability was set to 1 false alarm every 10 hours, and the true positive probability was set to 90%.

VI. Conclusion

A large panel monitor using straw detector technology with distinct advantages over ^{3}He detectors is proposed for long range detection of small sources in an unknown but uniform background. An algorithm is presented that uses the rotating panel detector's angular response data to successfully localize very small signals. The algorithm's operation was demonstrated with a small-scale prototype detector, in laboratory experiments. Figs. 12 and 13 illustrate how the proposed method makes successful detections even when a source is not evident in the count rate data.

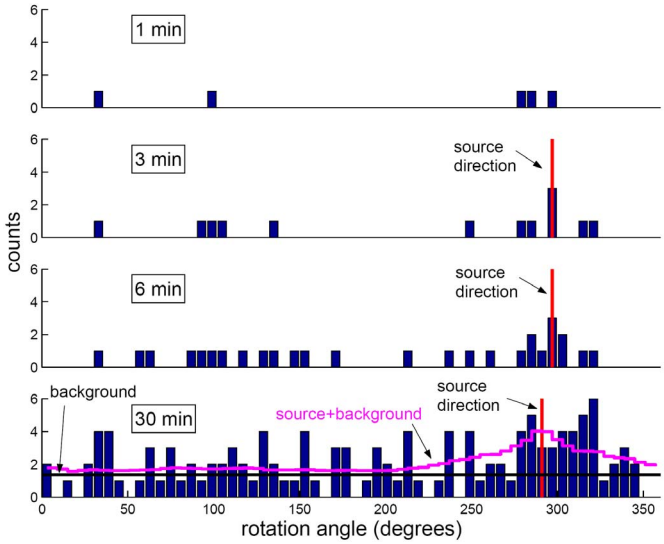

Fig. 13. Cumulative counts collected in the small-scale, rotating monitor, in an experiment involving a 0.37 μg ^{252}Cf source located 10.2 m away, and behind walls/furniture. Following processing with the proposed algorithm, a confident detection was declared at 3 min, for a source located at a direction of 297 degrees (red line). The false alarm probability was set to 1 false alarm every 10 hours, and the true positive probability was set to 90%.

Appendix

A. Derivation of (2)

Based on (1) we can write,

$$f_i = a' \cdot yt_i + BG_i \tag{5}$$

where $yt_i = yt_i(\theta_i+b)$ is the template data for angle θ_i+b, b is a shift in the angle, and BG_i the gamma background rate. We have three unknowns here: the constant parameters a', b and BG_i. We can eliminate one by normalizing the above, as such

$$f_i = a \cdot yt_i / \Sigma(yt_i) + c \cdot BG_i / \Sigma(BG_i) \tag{6}$$

Since BG_i is constant for all i's, the last term is simply $c \cdot (1/30)$, and then if we sum f_i over all i's we get

$$\begin{aligned} \Sigma(f_i) &= a \cdot \Sigma(yt_i)/\Sigma\,(yt_i) + c \cdot 30 \cdot (1/30) \\ &= a+c. \end{aligned} \tag{7}$$

But $\Sigma(f_i) = \Sigma(y_i)$ is known, so we can express c as $c=\Sigma(y_i)-a$. Now (6) becomes

$$f_i = a \cdot yt_i / \Sigma(yt_i) + (\Sigma(y_i)-a) \cdot (1/30), \tag{2}$$

and we now have only two parameters, namely a and b. The

first term on the right hand side of the equation is the net signal, and the second term is the background.

B. Error analysis

If a_0 and b_0 are the parameter values that minimize χ^2 of (3), the standard deviation in the parameter estimates, σ_a and σ_b, is computed using the formula

$$\chi^2 (a_0+\sigma_a, b_0+\sigma_b) = \min(\chi^2)+2.41. \quad (8)$$

The constant 2.41 is the value of χ^2 that is exceeded with a probability of 70% for 2 degrees of freedom (2 parameters).

REFERENCES

[1] J. L. Lacy, A. Athanasiades, N. N. Shehad, C. S. Martin, and L. Sun, "Performance of 1 Meter Straw Detector for High Rate Neutron Imaging," *IEEE Nuclear Science Symposium Conference Record*, vol. 1, pp. 20-26, 2006.

[2] A. Athanasiades, N. N. Shehad, L. Sun, T. D. Lyons, C. S. Martin, L. Bu, and J. L. Lacy, "High sensitivity portable neutron detector for fissile materials detection," *IEEE Nuclear Science Symposium Conference Record*, vol. 2, pp. 1009-1013, 2005.

[3] R. C. Runkle, T. M. Mercier, K. K. Anderson, and D. K. Carlson, "Point Source Detection and Characterization for Vehicle Radiation Portal Monitors", *IEEE Tans. Nucl. Sci.*, vol. 52, no. 6, pp. 3020-3025, 2005.